International Symposium
On Turbulence and Shear Flow
Phenomena (TSFP-9)
June 30 - July 3, 2015 *Melbourne, Australia*

LARGE EDDY SIMULATION OF TURBULENT FLOW OVER ARRAYS OF WALL-MOUNTED CYLINDERS AS VEGETATION MODEL CANOPY

Chao Yan
Department of Engineering Mechanics
Tsinghua University
Beijing, China
yan-c11@mails.tsinghua.edu.cn

Gui-Xiang Cui
Department of Engineering Mechanics
Tsinghua University
Beijing, China
cgx@tsinghua.edu.cn

Zhao-Shun Zhang
Department of Engineering Mechanics
Tsinghua University
Beijing, China
demzzs@mail.tsinghua.edu.cn

ABSTRACT

Large eddy simulations (LES) of turbulent flow over two kinds of vegetation-like model canopies are conducted here, including flow over a shallow submerged aquatic canopy and flow over a terrestrial canopy, with the aim of visualizing the underlying fluid dynamical processes within vegetation canopies. A physical model that fully resolves each vegetation element has been developed. The resulting mean flow and turbulence statistics show good agreement with measurements from previous experiment. Canopy-scale structures within vegetation canopies penetrate only a fraction of the canopy layer, which divide the flow field into three different regions based on the relative importance of canopy- and stem-scale turbulence structures. Stem-scale vortices dominate at the ground, while canopy-scale prevail above the canopy layer. In the intermediate region, stem-scale turbulence will interfere with canopy-layer turbulence, which makes the momentum transport more efficient.

INTRODUCTION

Vegetation is known to exert notable influences on its surrounding terrestrial or aquatic environments, such as regulating air quality and reducing soil erosion in local regions. Yet the influences have not been fully understood, since strongly complex turbulent flow prevails within and above plant canopies. During the past three decades, considerable efforts have been spent to shed light upon the vegetation-enviroment interaction in respects of physical mechanisms, field experiments and numerical simulations. For comprehensive overviews on this subject, please refer to Belcher et al. (2012) and Nepf (2012a).

As for numerical simulation, consideration of detail plant morphology remains unattainable since a natural vegetation canopy consists of assorted elements, such as leaves, twigs and branches. Hence, vegetation has long been considered as a source of flow resistance, and its effects were accounted for by adding a drag force term into the momentum equation. To further simplify the model, fairly large amounts of study focus on the exchange of scalar and momentum in horizontally uniform canopies, assuming that the canopy architecture varies only in the vertical direction (Cui and Neary, 2008; Dupont and Brunet, 2008). This one-dimensional treatment is the most practical approach for understanding the mean flow field in plant canopies. The discontinuity in drag prompts the appearance of an inflection point, which is the main cause of coherent structures that generate at the top of the canopy layer. A growing consensus exists today that better understanding of the environmental impact by vegetation requires an in-depth knowledge of flow structures (Nepf, 2012b). Recently, based on their LES study, Finnigan et al., (2009) proposed dual-hairpin shape eddies as the principal structures that dominate momentum and scalar transfer in the roughness sub-layer (RSL).

However, this model needs to be further improved, for it only took into account the influences of vegetation on the bulk flow while flow structures within the canopy were beyond reach. Apparently, the solid plant elements will introduce spatial heterogeneity to the flow field, leading to the failure of the assumption of homogeneous canopies. Therefore, many researchers turn to investigate turbulent flow over heterogeneous plant canopies, such as canopy edge (Belcher 2003). It has been demonstrated that spatial heterogeneity can produce complex flow patterns which differ significantly from that of horizontal homogeneous case. However, it is still unclear which canopy model is more appropriate.

In wind tunnel and flume experiments, vegetation canopies are usually treated as regular arrays of bluff bodies (Poggi et al., 2004; Böhm et al., 2013). Poggi et al. (2004)

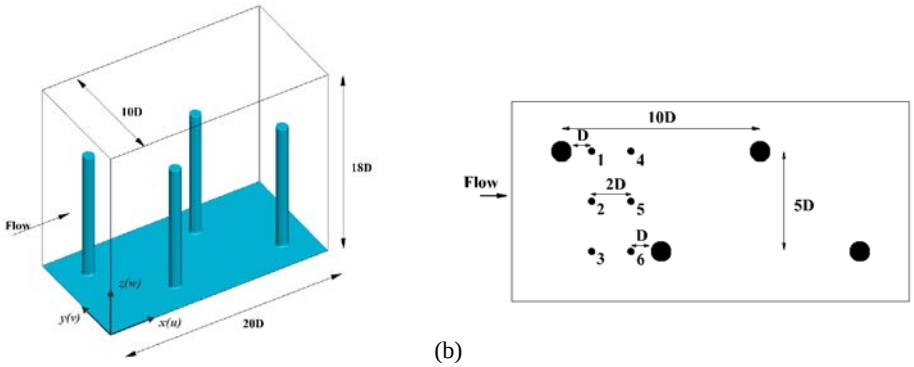

(a) (b)

Figure 1. Schematic of flow over submerged canopies (a) Computational domain and coordinate system; (b) Cylinder arrangement and monitoring locations

conducted some measurements in open channel flows with vegetation elements modelled as rigid circular cylinders and proposed that the dominant turbulent eddies associated with the instability of the inflection point are perturbed by the wake structure behind vegetation stems. Recent wind-tunnel experiment of (Böhm et al., 2013), in which each individual vegetation element is a combination of sphere-shaped tree crown and a cylindrical trunk, drew the similar conclusion. It is widely accepted that a better representation of the canopy architecture may contribute to revealing the underlying fluid mechanics.

The main targets of the present work are twofold. Firstly, we consider the statistical results of the flow to evaluate how well these models represent real vegetation canopy flows. Secondly, the effects of stem- and canopy-scale turbulence structure on the momentum transfer, which are of crucial importance for the explaination of the flow characteristics, will be depicted.

BASIC EQUATIONS AND NUMERICAL APPROACH

LES was employed to address such complex flow problems given its unparalleled role in providing spatial details and interpretng the measurements. The basic idea of LES is to solve directly for the resolved scales of motion, which are separated from the sub-grid scales by a spatial filter. Application of such filter to the incompressible Navier-Stokes equations yields:

$$\frac{\partial u_i}{\partial x_i} = 0 \tag{1}$$

$$\frac{\partial u_i}{\partial t} + \frac{\partial \left(u_i u_j\right)}{\partial x_j} = -\frac{1}{\rho}\frac{\partial p}{\partial x_i} + \frac{\partial}{\partial x_j}\left(\nu \frac{\partial u_i}{\partial x_j} + \tau_{ij}\right) + f_i \tag{2}$$

where ρ and ν are fluid density and kinematic viscosity respectively, u_i represents the filtered velocity component in the x_i (i =1,2,3) direction, f_i is the momentum forcing term. The subgrid-scale (SGS) stress tensor τ_{ij} reflects the effect of the subgrid scales upon the resolved scales, and is modelled using the Lagrangian dynamic model.

The Navier-Stokes equations (1) and (2) were discretized on a collocated mesh in the framework of finite volume method. The convective terms are discretized using the QUICK scheme, while the diffusive terms are discretized using a second order central difference scheme. The SIMPLE algorithm and momentum interpolation are employed to solve the pressure and velocity coupling. On account for the challenges for the modelling arising from the random distribution of plants, the immersed boundary method (IBM) was adopted considering its ability to simplify flow problems associated with the grid generation. The LES code is highly paralleled in the horizontal directions to reduce the computational load. Further details about the numerical methods and validation can be found in Yan et al. (2015).

SIMULATION SET-UP

LES of water flow over a shallow submerged aquatic canopy, with water depth (H) to vegetation height (h) at the ratio of H/h = 1.5 and frontal area per unit ground λ = 0.48, was conducted. The canopy is modelled as an array of wall-mounted cylinders. The box-shaped computational domain incorporates 4 circular cylinders planted in a staggered arrangement (shown in Figure 1), together with six monitoring locations which are identical to the experimental measurement locations of Liu et al. (2008). The mesh is locally refined near the ground and the top of canopy layer to resolve the steep variation of mean flow and turbulence statistics, while stretched outside in the vertical direction. 24 grid points are uniformly distributed within the cylinder diameter, while the grid is stretched outside in both the streamwise and lateral directions. Stoesser et al. (2009) recently performed the LES of flow over arrays of cylinders with a resolution of 80 grids per cylinder. The computational domain used in SSRD is four times as large as that in this case. The detailed comparison between the current results and published data will be given in the next section.

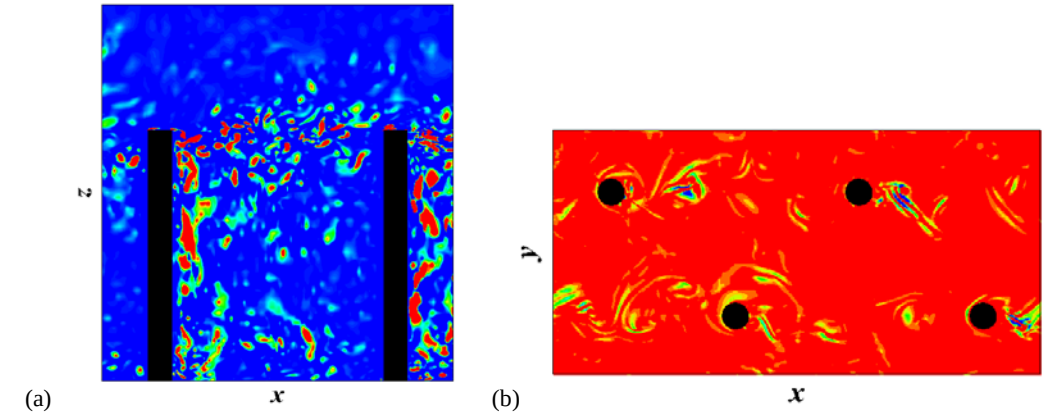

Figure 2. Isosurfaces of instantaneous Q-criterion in a (a) vertical plane; (b) near-bed horizontal plane.

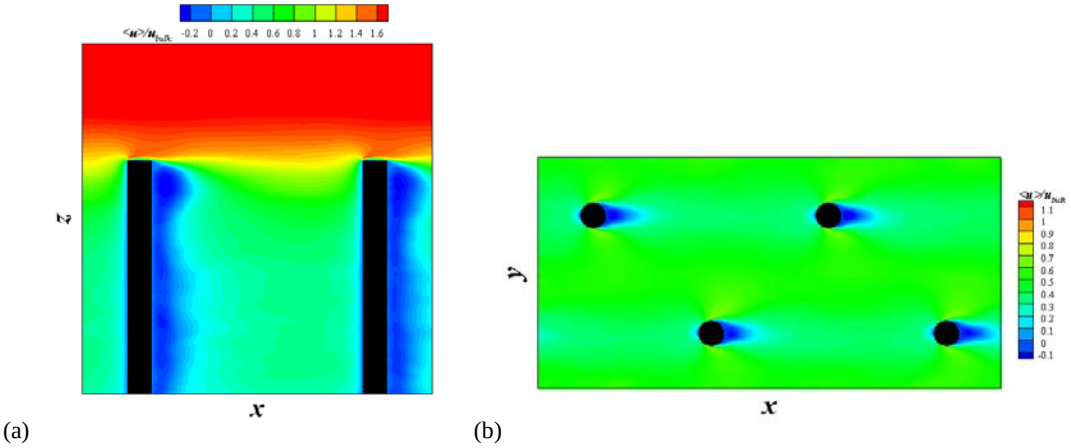

Figure 3. Contours of mean streamwise velocity field in a (a) vertical plane and (b) near bed horizontal plane

No-slip boundary conditions are applied at the surfaces of solid plant elements via IBM, while free-slip condition is imposed at the top of the computational domain. Periodic boundary conditions are imposed in the horizontal directions to simulate an infinite array. The friction Reynolds number is estimated to be approximately $\mathrm{Re}_\tau = u_\tau H/\nu = 4{,}650$, based on total shear velocity u_τ and water depth H. Here, the shear velocity is defined as $u_\tau = [g(H-d)I_e]^{1/2}$, where I_e is the energy gradient and d is the zero-plane displacement height. For shallow submerge canopis, this indicator constitutes a more appropriate scaling velocity to collapse turbulence statistics of vegetated flow (Nepf and Vivoni, 2000).

The simulation is initialized with logrithmic velocity profile adding by random fluctuations. When the flow field has reached the state of statistical equilibrium, flow quantities are averaged over 40 non-dimensional time units to obtain the statistical results.

INSTANTANEOUS FLOW FIELD VISUALIZATIONS

Figure 2 presents the isosurface of the Galilean invariant Q in a x-z plane that cut through the middle of cylinder and a x-y plane that is contiguous to the bed.

At the top of the canpy layer, vortical structures are constantly generated at the sharp corner of the canopy interface. While these vortices convect downstream, they penetrate a finite distance into the canopy layer, as shown in Figure 2(a) that most structures are mainly distributed in the upper canopy layer.

In the lower canopy layer, the flow field in the selected horizonal plane highlights the two separating shear layers on both sides of the cylinders, leading to the development of Karman vortex streets in the cylinder wakes. The scale of the primary vortex in this layer is comparable to the cylinder diameter. In the mean sense, an approximately symmetric counter-rotating vortices develops behind the cylinders (see Figure 3).

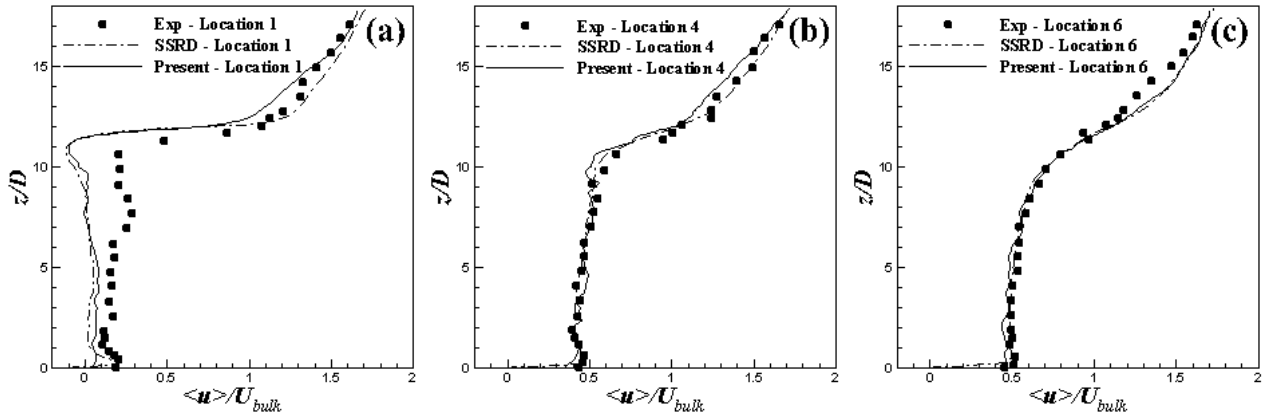

Figure 4. Vertical profiles of the mean streamwise velocity at the three different monitoring locations (1, 4, and 6) compared against previously published experimental and numerical results.

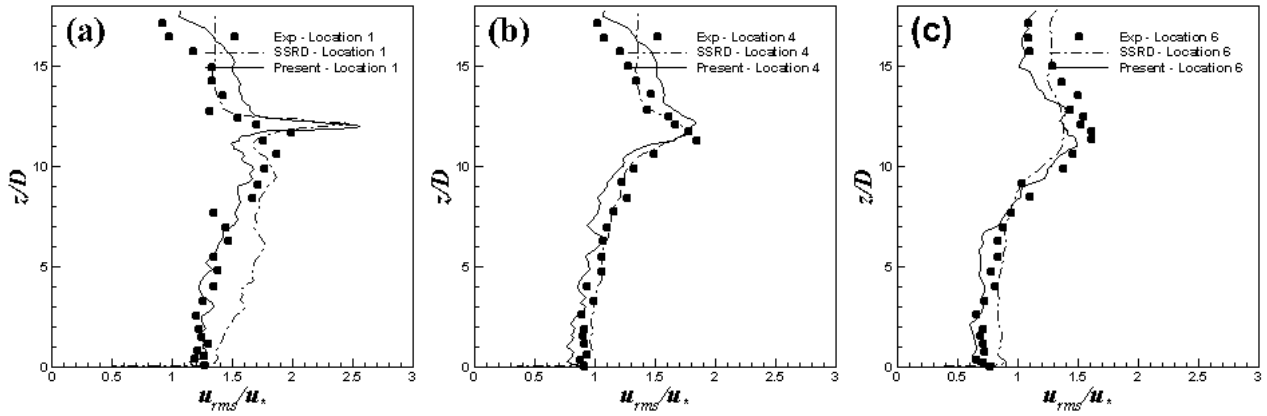

Figure 5. Vertical profiles of the streamwise turbulence intensity at the six monitoring locations (1, 4, and 6) compared against previously published experimental and numerical results.

MEAN FLOW AND TURULENCE STATISTICS

The vertical profiles of mean velocities and turbulence intensities at different detecting points were compared with laboratory data. The numerical results agree well with experimental measurements (see sample results shown in Figures 4 and 5 along three representative locations). Vertical coordinate has been normalized by canopy height h, as well as all velocity moments by either the canopy-top mean wind u(h) or the canopy top friction velocity. The simulation data extracted from Stoesser et al. (2009) have also benn included (refered to as SSRD) here for comparison.

Some discrepancies exist for the streamwise velocity within the canopy sub-layer. The LES fails to predict the formation of near bed velocity bulge, possibly because the subgrid-scale parameterization is incapable of taking spectral shortcut into account (Finnigan, 2000). In addition, the calculated velocity in free stream region (locations 2 and 5) seems to be smaller than that of measurements. The reason for this can properly be ascribed to the relative larger local friction velocity u_* than that of wake region (locations 1, 3, 4 and 6). The larger local friction velocity u_* is, the greater wall units $y^+ = u_* y/\nu$ will be, thus invalidating the log-law wall model in local regions.

As shown in Figure 4, time-averaged streamwise velocity distribution at all monitoring locations resemble a mixing-layer profile without exception. This is consistent with mixing-layer analogy (Finnigan, 2000). Nearly constant velocity prevails within the canopy sub-layer while a logarithmic profile develops above. The inflection point near the top of the cylinder array is susceptible to Kelvin-Helmholtz instabilities, leading to the generation of clockwise canopy-scale vortices. Once formed, the canopy-scale structure governs the momentum transfer at the canopy interface. These can be confirmed by examining the vertical

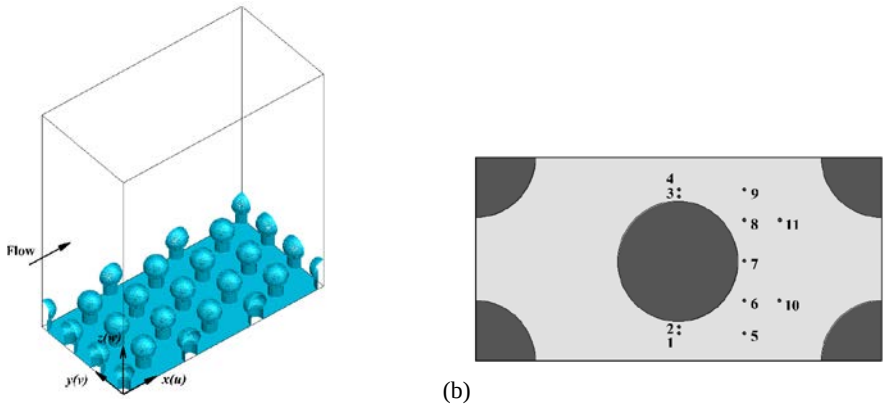

(a) (b)

Figure 6. Schematic of air flow over Black Forest Model canopies (a) computational domain and coordinate system; (b) locations of point measurements in a unit.

velocity profiles (not shown).

Time-aveaged vertical velocity in the wake region is almost positive along the whole water depth except near the top of the canopy sub-layer, indicating that downward flow is localized to the region at canopy interface in the wake region. Under the continuity constraint, fluid in the free stream region will be transported to the upper field which conforms to the calculated results, thus supporting the argument that canopy-scale vortices play a dominant role in momentum transfer at canopy interface.

In consequence, the stem- and canopy-scale turbulence increase the streamwise and vertical turbulence intensities throughout most of the flow depth, except in the vicinity of the bed, where it is almost constant (see Figure 5). It is worth mentioning that, although with a relatively sparse grid, the turbulent second-order moments show better agreement with laboratory measurements than the numerical results of SSRD. Profiles of streamwise and vertical turbulence intensities at all six monitoring locations reach a maximum near the top of the cylinder array, and decrease toward the bed and the free surface. The constant turbulence intensities region near the bed can be properly related to the mixed effect exerted solely by stem-scale structure which tends to be isotropic. This result implies that the canopy-scale structure reached a fixed penetration into the canopy, which is consistent with the descriptions given above.

In view of the turbulence intensities distribution, the flow field can be decomposed into three distinct zones:

• The lowermost zone ($z/h < 1/4$) in which the flow field is dominated by stem-scale strucutures associated with Karman vortex streets.

• The uppermost zone ($z/h > 1$) in which the flow field is dominated by canopy-scale structures arised from Kelvin-Helmholtz instability.

• The intermediate zone ($1/4 \leq z/h < 1$) in which the flow field is subjected to the combined effect by the stem- and canopy-scale structures.

FLOW OVER BLACK FOREST MODEL CANOPY

As a further step, an improved vegetation model, refered to as Black Forest Model by Böhm et al. (2013), has been established to represent real terrestrial vegetation. Each vegetation element consists of a cylindrical trunk and a spherical crown.

The simulation was conducted under conditions that match the wind tunnel experiment. The computational domain extends 14.2h×7.1h×8h in streamwise, lateral and vertical directions, which is large enough to allow for the evolution of the roughness layer and the dominant coherent structures contained therein. Flow over this terrestrial canopy model can be regarded as deeply submerged canopy. For clearness, only one fourth of the whole computational domain is shown in Figure 6, as well as eleven monitoring points in a unit of the array. The frontal area per unit ground $\lambda_f = 0.37$ and plan area per unit ground $\lambda p = 0.28$, which are almost identical to that of the wind-tunnel experiment. Uniform grids are used in the horizontal direction, with 24 grid points distributed within the sphere diameter. The flow is driven by a constant streamwise pressure gradient.

The corresponding roughness Reynolds number Re_τ, based on total shear velocity u_τ and canopy height h, was estimated to be approximately $Re_\tau = u_\tau h/\nu \approx 1120$, which is comparable to that of experiment.

Figure 7 shows the vertical profile of normalized space-time averaged drag force FD, which is calculated using both Reynolds stress and dispersive stress gradients. The drag coefficient is in agreement with that of wind-tunnel experiment. Details of the mean flow field and turbulence statistics will be in future studies.

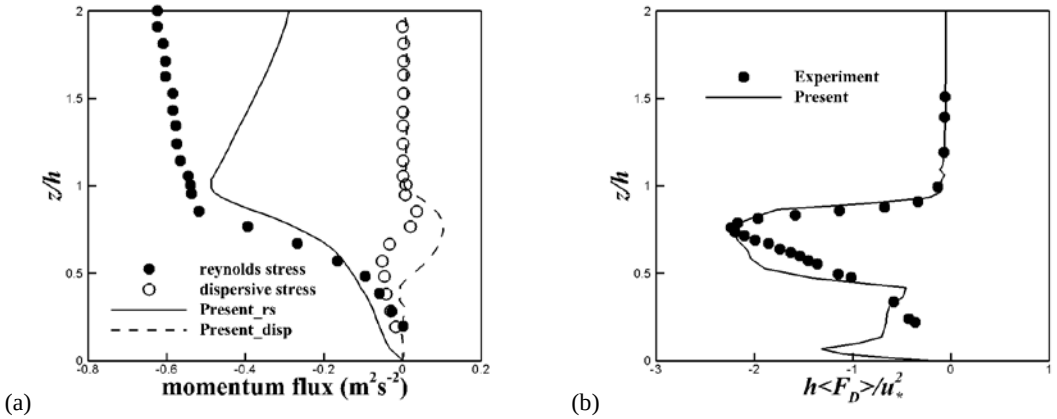

Figure 7. comparison of (a) Reynolds stress and dispersive stress; (b) Normalized space-time averaged drag force

CONCLUDING REMARKS

Turbulent flow over idealized vegetation-like canopy models are numerically simulated by means of large eddy simulation (LES). Experimentally observed features of flow through vegetation, such as the inflection points and maximum turbulence intensities at the top of the canopy sub-layer, were well simulated. The flow field can be categorized into three distinct regions, each characterized by turbulence structures of different scales. The canopy-scale vortices dominate the vertical transport at the canopy interface, interacting with stem-scale vortices in the mean time. The relative importance of canopy- and stem-scale structures varies with canopy density which requires further examination on the inter-connection between canopy density and flow statistics.

ACKNOWLEDGMENTS

The work was supported by National Natural Science Foundation of China under Grant [11132005]. The authors would also like to thank Tsinghua National Laboratory for Information Science and Technology for the support in parallel computing.

REFERENCES

Belcher, S. E., Jerram, N., and Hunt, J. C. R., 2003, "Adjustment of a turbulent boundary layer to a canopy of roughness elements", *Journal of Fluid Mechanics*, Vol. 488, pp. 369-398.

Belcher, S. E., Harman, I. N., and Finnigan, J. J., 2012, "The Wind in the Willows: Flows in Forest Canopies in Complex Terrain", *Annual Review of Fluid Mechanics*, Vol. 44, pp. 479-504.

Böhm, M., Finnigan, J. J., Raupach, M. R., and Hughes, D., 2013, "Turbulence Structure Within and Above a Canopy of Bluff Elements", *Boundary-Layer Meteorology*, Vol. 146, pp. 393-419.

Cui, J., and Neary, V. S., 2008, "LES study of turbulent flows with submerged vegetation", *Journal of Hydraulic Research*, Vol. 46, pp. 307-316.

Dupont, S., and Brunet, Y., 2008, "Influence of foliar density profile on canopy flow: A large-eddy simulation study", *Agricultural and Forest Meteorology*, Vol. 148, pp. 976-990.

Finnigan, J. J., 2000, "Turbulence in plant canopies", *Annual Review of Fluid Mechanics*, Vol. 32, pp. 519-571.

Finnigan, J., Shaw, R., and Patton, E., 2009, "Turbulence structure above a vegetation canopy", *Journal of Fluid Mechanics*, Vol. 637, pp. 387-424.

Liu, D., Diplas, P., Fairbanks, J. D., and Hodges, C. C., 2008, "An experimental study of flow through rigid vegetation", *Journal of Geophysical Research: Earth Surface*, Vol. 113, pp. F04015.

Nepf, H. M., 2012a, "Flow and Transport in Regions with Aquatic Vegetation", *Annual Review of Fluid Mechanics*, Vol. 44, pp. 123-142.

Nepf, H. M., 2012b, "Hydrodynamics of vegetated channels", *Journal of Hydraulic Research*, Vol. 50, pp. 262-279.

Nepf, H. M., and Vivoni, E. R., 2000, "Flow structure in depth-limited, vegetated flow", *Journal of Geophysical Research*, Vol. 105, pp. 28547-28557.

Poggi, D., Porporato, A., Ridolfi, L., Albertson J. D., and Katul G. G., 2004, "The Effect of Vegetation Density on Canopy Sub-Layer Turbulence", *Boundary-Layer Meteorology*, Vol. 111, pp. 565-587.

Stoesser, T., Salvador, G. P., Rodi, W., and Diplas, P., 2009, "Large Eddy Simulation of Turbulent Flow Through Submerged Vegetation", *Transport in Porous Media*, Vol. 78, pp. 347-365.

Yan, C., Huang, W. X., Cui, G. X., Xu C., and Zhang Z. S., 2015, "A ghost-cell immersed boundary method for large eddy simulation of flows in complex geometries", *International Journal of Computational Fluid Dynamics*, Vol. 29, pp. 12-25.